A PROBABILISTIC INTERFERENCE DISTRIBUTION MODEL ENCOMPASSING CELLULAR LOS AND NLOS MMWAVE PROPAGATION

Hussain Elkotby and Mai Vu

Department of Electrical and Computer Engineering, Tufts University, Medford, MA, USA
Emails: Hussain.Elkotby@Tufts.edu, Mai.Vu@Tufts.edu

ABSTRACT

We propose a novel probabilistic model for the interference power distributions in a cellular network employing MIMO beamforming in mmWave spectrum. Considering both line-of-sight (LOS) and non-line-of-sight (NLOS) propagations, we use the Gamma distribution for LOS interference power, and propose a mixture of the Inverse Gaussian and Inverse Weibull distributions for the NLOS interference power. For the NLOS mixture model, an expectation maximization algorithm is developed using both analytical moment matching and maximum likelihood estimation. The composite probabilistic model is tested against simulation data obtained from a stochastic geometry based cellular network and demonstrates low relative entropy (Kullback-Leibler distances) for a wide range of practical mmWave path loss and shadowing values.

Index Terms— interference models; mixture distribution.

1. INTRODUCTION

The underutilized mmWave bands (3-300 GHz) have been the focus of current research as a promising candidate for 5G systems. The bands are expected to solve the current problem of wireless spectrum scarcity coupled with the predicted exponential increase in capacity demand [1–4]. Traditionally, mmWave bands are considered for backhaul in cellular systems, but not for cellular access. Recent trials, however, show that nodes equipped with a large number of antennas can successfully compensate for the high path loss and establish high-rate communication over short distances (100-200m) [2, 4]. As a result, mmWave is being considered for cellular access networks with short cell radius.

Smaller cell radii lead to dense base station (BS) deployments. Even under beamforming, these high BS and user densities can drive the cellular networks to be more interference rather than noise limited. While many-element adaptive arrays can boost the received signal power and hence reduce the impact of out-of-cell interference [3, 5], interference characterization still plays an important role in evaluating and predicting the dense mmWave networks performance.

mmWave cellular systems differ considerably from conventional systems due to the particular channel characteristics. Not only the propagation path loss is much higher with distance, but measurement results show that mmWave sensitivity to blockages also leads to severe shadowing effects and to different path loss characteristics between LOS and NLOS links [1, 4, 6, 7]. Shadowing is of particular concerns and cannot be ignored in urban environments where mmWave is predicted to have wide usage [8].

In our recent work [9], we modeled the NLOS interference at the base station (BS) in an uplink communication scenario, outside the approximated LOS ball region as in [10]. In this work, we model the interference power at a receiver that can be located anywhere in a cell of a fixed radius. We further revoke the LOS ball region approximation and instead consider a probability function $p_{los}(d)$ that defines the probability a link of length d is LOS [11]. We show, by testing against simulation data obtained from a stochastic geometry based cellular network, that the Gamma distribution and the mixture of the Inverse Gaussian (IG) and Inverse Weibull (IW) distributions can accurately model the LOS and NLOS interference power, respectively, irrespective of the receiving node location. We consider either moment matching (MM) or maximum likelihood estimation (MLE) to estimate the Gamma distribution parameters and a combination of MM and MLE to estimate the mixture model parameters.

2. NETWORK AND CHANNEL MODELS

2.1. Network model based on stochastic geometry

Consider a cellular system consisting of multiple cells with a typical cell of average radius R_0 under consideration. We consider downlink transmissions in this paper and focus on the interference at a user equipment (UE) located at a distance D from the BS at the origin. In this cellular system, each cell has a single BS that is equipped with N_{BS} antennas and serves multiple UEs. Each UE is equipped with N_{UE} antennas and uses a distinct resource block in each cell. Each UE suffers from out-of-cell interference due to frequency reuse in all other cells. Further, we assume that each UE is served by the single BS closest to that user.

We model the BSs in different cells contending for the same resource block and causing interference to each other as being distributed on a two-dimensional plane according to a homogeneous and stationary Poisson point process (p.p.p.)

Φ with intensity λ_1. Connection from each BS can either be a LOS or NLOS to the UE under consideration according to the LOS probability function $p(r)$ that defines the probability that a link of length r is LOS. Assuming independence in LOS probabilities among different links, we can represent the two BSs point processes Φ_L and Φ_N corresponding to the LOS and NLOS propagations as two independent non-homogeneous p.p.p. with intensity functions $p(r)\lambda_1$ and $(1-p(r))\lambda_1$, respectively.

2.2. mmWave channel propagation model

We consider a complete channel model with shadowing, path loss and small scale fading. We also consider the probabilistic LOS and NLOS characteristics of a mmWave communication link. As such, we express a typical MIMO channel with Tx-Rx distance r in the following form:

$$\mathbf{H} = \sqrt{l(r)}\tilde{\mathbf{H}} \tag{1}$$

where random matrix $\tilde{\mathbf{H}}$ captures the effects of small scale fading, and function $l(r)$ captures the large scale fading. Rician distribution has been used to model the small-scale fading distribution [12]. However, in this paper, we adopt the model in [13] where each element in $\tilde{\mathbf{H}}$ is i.i.d. $\mathcal{CN}(0,1)$. Consideration of a directional or Rician channel model will be carried out in future work.

The large scale fading function $l(r)$ captures both LOS and NLOS propagation probabilistically as follows:

$$l(r) \;=\; \mathbb{B}\left(p(r)\right) L_l \beta_l r^{-\alpha_l} + \left(1-\mathbb{B}\left(p(r)\right)\right) L_n \beta_n r^{-\alpha_n} \tag{2}$$

where $\mathbb{B}(x)$ is a Bernoulli random variable with parameter x representing the LOS probability; $L_l \sim log(0,\sigma_l)$ and $L_n \sim log(0,\sigma_n)$ are log-normal random variables with standard deviations σ_l dB and σ_n dB that capture the shadowing effect of LOS and NLOS propagations, respectively; and $\{\alpha_l,\alpha_n\}$ and $\{\beta_l,\beta_n\}$ are the LOS and NLOS pathloss exponents and intercepts [14].

In this paper we consider the measurement based LOS probability introduced in [11] as

$$p(r) = \left[\min\left(\frac{r_{BP}}{r},1\right)\left(1-e^{-r/\alpha}\right)+e^{-r/\alpha}\right]^2 \tag{3}$$

where r_{BP} is the breakpoint distance at which the LOS probability is no longer equal to 1, and α is a decay parameter.

3. INTERFERENCE VECTOR FORMULATION

For the purpose of modeling network-wide interference, we emphasize that the distribution of interference is independent of the beamforming scheme employed. This condition is realistic in most practical scenarios. We consider the downlink interference at a UE from all active BSs at the same resource block as the considered UE.

For the k^{th} interfering BS, denote its unit-norm beamforming vector as $\mathbf{w}_k \in \mathbb{C}^{N_{\text{UE}}\times 1}$. This beamforming vector depends on the direct channel between the k^{th} active BS and its served UE and hence is independent of the interference channel $\mathbf{H}_k$. Then, the effective interference vector from the k^{th} interfering active BS is

$$\mathbf{h}_k = \mathbf{H}_k\mathbf{w}_k = \sqrt{l\left(\|\mathbf{z}_k-\mathbf{t}_0\|_2\right)}\tilde{\mathbf{H}}_k\mathbf{w}_k = \sqrt{l\left(\|\mathbf{z}_k-\mathbf{t}_0\|_2\right)}\tilde{\mathbf{h}}_k, \tag{4}$$

where $\mathbf{t}_0$ and $\mathbf{z}_k$ are the 2-D locations of the considered UE and the k^{th} interfering BS in Φ with respect to the origin; and $\tilde{\mathbf{h}}_k$ is a random vector with i.i.d. elements as $\mathcal{CN}(0,1)$.

The interference vector received at the considered UE from all active BSs can then be expressed as

$$\mathbf{v}_0 = \sum_k \mathbf{h}_k x_k = \sum_{\mathbf{z}_k\in\Phi} \sqrt{P_k l\left(\|\mathbf{z}_k-\mathbf{t}_0\|_2\right)}\tilde{\mathbf{h}}_k U_k. \tag{5}$$

The transmitted signal $x_k = \sqrt{P_k}U_k$ where P_k represents the total allocated power and U_k is a transmit symbol of distribution $\mathcal{CN}(0,1)$.

For each realization of the interferers locations, the out-of-cell interference in Eq. (5) can be modeled as $\mathcal{CN}(\mathbf{0},\mathbf{Q}_0)$. Covariance matrix $\mathbf{Q}_0$ is symmetric with diagonal elements representing the interference power at each receiving antenna element, and the off-diagonal elements representing the correlation among interference signals. However, the correlation is found to be weak and negligible [9] and hence we focus on modeling the diagonal elements of $\mathbf{Q}_0$.

4. INTERFERENCE POWER PER ANTENNA ELEMENT

4.1. Interference power moments

The diagonal elements of $\mathbf{Q}_0$ form a random vector of independent elements, each element is expressed as

$$q_0 = \sum_{\mathbf{z}_k\in\Phi_l} l\left(\|\mathbf{z}_k-\mathbf{t}_0\|_2\right) g_k P_k + \sum_{\mathbf{z}_k\in\Phi_n} l\left(\|\mathbf{z}_k-\mathbf{t}_0\|_2\right) g_k P_k, \tag{7}$$

where g_k are all i.i.d. $\exp(1)$ and represent the power gain of the Rayleigh channel fading from the k^{th} interferer.

Lemma 1 below characterizes the first two moments of the interference power q_0 at each receiving antenna, based on the stochastic geometry network model.

Lemma 1 (Interference Power Moments)**.** *For network-wide employment of MIMO beamforming, the interference power at each antenna of the interfered receiver has the statistics:*

$$\mathbb{E}\left[q_0\right] = \mu_l + \mu_n, \quad var\left[q_0\right] = \nu_l + \nu_n. \tag{8}$$

Here $\{\mu_l,\mu_n\}$ and $\{\nu_l,\nu_n\}$ represent the mean and variance of interference power from LOS and NLOS interferers as

$$\mu_i(D) = \zeta_i \int_0^{2\pi}\int_{R_c}^{\infty} p_i\left(d(r,\phi,D)\right) d(r,\phi,D)^{-\alpha_i} r\,dr\,d\phi, \tag{9}$$

$$\nu_i(D) = \tilde{\zeta}_i \int_0^{2\pi}\int_{R_c}^{\infty} p_i\left(d(r,\phi,D)\right) d(r,\phi,D)^{-2\alpha_i} r\,dr\,d\phi, \tag{10}$$

where $i\in\{l,n\}$; and $d(r,\phi,D)$, $p_l(x)$, $p_n(x)$, ζ_i, and $\tilde{\zeta}_i$ are defined as

$$d(r,\phi,D) = \sqrt{r^2+D^2-2rD\cos(\phi)},$$
$$p_l(x) = p(x), \qquad p_n(x) = 1-p(x),$$
$$\zeta_i = \lambda_1 P_k \beta_i \mathbb{E}[L_i], \quad \tilde{\zeta}_i = 2\lambda_1 P_k^2 \beta_i^2 \mathbb{E}[L_i^2]. \tag{11}$$

Proof. Omitted due to space, see [15] for details. □

1.	**Initialization:**	Initialize $w_j^{(0)}$, $\lambda^{(0)}$, and $c^{(0)}$, $j \in \{1,2\}$, and compute the initial log-likelihood: $$L^{(0)} = \frac{1}{n}\sum_{i=1}^{n} \log\left(w_1^{(0)} f_{\gamma_{IG}}\left(y_i|\lambda^{(0)}\right) + w_2^{(0)} f_{\gamma_{IW}}\left(y_i|c^{(0)}\right)\right). \quad (6)$$
2.	**E-step:**	Compute $\gamma_{ij}^{(m)}$ as given in Eq. (19) and $n_j^{(m)} = \sum_{i=1}^{n} \gamma_{ij}^{(m)}$.
3.	**M-step:**	Compute the new estimate for $w_j^{(m+1)}$, $\lambda^{(m+1)}$, and $c^{(m+1)}$, $j \in \{1,2\}$ as given in Eqs. (20), and (21).
4.	**Convergence check:**	Compute the new log-likelihood function $L^{(m+1)}$.
	Return to 2 if $\lvert L^{(m+1)} - L^{(m)}\rvert \geq \delta$ for a preset threshold δ; **Otherwise** end the algorithm.	

Algorithm 1. Mixture MLE Model EM Algorithm

4.2. Modeled interference distributions

The LOS and NLOS interference components are modeled separately. For the LOS interference, we use the Gamma distribution and apply moment matching (MM) to estimate its parameters. For the NLOS interference, we propose a distribution as a mixture of Inverse Gaussian (IG) and Inverse Weibull (IW), and apply MLE to estimate its parameters. To simplify the mixture distribution parameters estimation, however, we use MM first to estimate a part of these parameters and then use MLE for the rest. We match the mean, $\mu_Y = \mu_n$, of the NLOS observed data set to that of each candidate distribution [16, 17]. This matching results in the scale parameters μ and b for the IG and IW distributions as

$$\mu = \mu_Y, \qquad b = \frac{\mu_Y}{\Gamma(1-1/c)}. \quad (12)$$

Next, we replace these expressions into the log-likelihood function for each candidate distribution, resulting in a single-parameter log-likelihood functions as

$$\log f_{\gamma_{IG}}(y|\lambda) = \frac{1}{2}\log\lambda - \frac{1}{2}\log 2\pi y^3 - \frac{\lambda}{2\mu_Y^2}\frac{(y-\mu_Y)^2}{y}, \quad (13)$$

$$\log f_{\gamma_{IW}}(y|c) = \log\frac{\mu_Y^c c}{\Gamma(1-1/c)^c y^{(c+1)}} - \left(\frac{\mu_Y}{\Gamma(1-1/c)}\right)^c y^{-c}, \quad (14)$$

where $\Gamma(t)$ is the Gamma function, λ and c are the shape parameters of the IG and IW distribution.

5. LOS AND NLOS INTERFERENCE MODELS

5.1. LOS Interference Model

We note that the LOS probability function $p(r)$ as in Eq. (3) is a decreasing function of r, which means that only interferers in a limited area have significant contribution to the LOS interference. This suggests that the LOS interference power distribution has considerable components around 0. Hence, we consider the Gamma distribution in modeling the LOS interference power as

$$\gamma_G(D) = \begin{cases} 0 & \text{with probability } p_0(D); \\ \tilde{\gamma}_G(D) & \text{with probability } 1-p_0(D), \end{cases} \quad (15)$$

where $p_0(D)$ is the probability that the LOS interference power is 0 and $\tilde{\gamma}_G(D)$ is a Gamma distribution with its parameters estimated using MLE or MM as in [18, 19] as

$$k_G = \frac{\tilde{\mu}_l^2(D)}{\tilde{\nu}_l(D)}, \qquad \theta_G = \frac{\tilde{\nu}_l(D)}{\tilde{\mu}_l(D)}, \quad \text{where} \quad (16)$$

$$\tilde{\mu}_l(D) = \frac{\mu_l(D)}{1-p_0(D)}, \tilde{\nu}_l(D) = \frac{\nu_l(D)+\mu_l^2(D)}{1-p_0(D)} - \tilde{\mu}_l^2(D). \quad (17)$$

where μ_l and ν_l are the mean and variance of the distribution to be fitted into a Gamma distribution.

5.2. NLOS Mixture Interference Model

The increasing NLOS probability function $1-p(r)$ suggests that the NLOS interferers occupy an infinite area. This implies that the NLOS interference components around 0 have very low probability. Hence, we consider a heavy-tail distribution that is a weighted mixture of both the IG and IW distributions. We can leverage MM to represent the mixture model as a 3-parameter distribution as follows.

Theorem 1. *Given a data set Y, the probability density function of the mixture interference model can be written as*

$$f_Y(y|\theta) = w_1 f_{\gamma_{IG}}(y|\lambda) + w_2 f_{\gamma_{IW}}(y|c), \quad (18)$$

where $\{w_1, w_2 : w_1 + w_2 = 1\}$ are the weight parameters for mixing the IG and IW distributions and $f_{\gamma_{IG}}(y|\lambda)$ and $f_{\gamma_{IW}}(y|c)$ are as given in Eqs. (13) *and* (14) *with the scale parameters obtained through moment matching first as in* (12)*. This mixture model is a 3-parameter distribution with the parameter set as $\theta = \{w_1, \lambda, c\}$.*

Given n observations $y_i, i \in \{1, 2, ..., n\}$, we use the EM algorithm developed in [9] to estimate the 3 parameters of this mixture distribution. The algorithm is summarized in Alg. 1 with the responsibility function $\gamma_{ij}^{(m)}$, representing our guess at the m^{th} iteration of the probability that the i^{th} sample belongs to the j^{th} distribution component, given as

$$\gamma_{ij}^{(m)} = \frac{w_j^{(m)}\phi_j(y_i|\theta_j^{(m)})}{\sum_{l=1}^{2} w_l^{(m)}\phi_l(y_i|\theta_l^{(m)})}, i \in \{1, ..., n\}, j \in \{1, 2\} \quad (19)$$

where $\phi_1(y|\theta_1) = f_{\gamma_{IG}}(y|\lambda)$ and $\phi_2(y|\theta_2) = f_{\gamma_{IW}}(y|c)$; and θ_1 and θ_2 represent the shape parameters λ and c. Then, the optimal parameters θ^* is found as in Theorem 2.

Theorem 2. *The optimal new estimate of $\theta^{(m+1)}$ of the mixture distribution at the m^{th} iteration are determined as*

$$w_j^{(m+1)} = \frac{n_j^{(m)}}{n}, j \in \{1,2\}, \lambda^{(m+1)} = \frac{n_1^{(m)}\mu_Y^2}{\sum_{i=1}^{n}\gamma_{i1}^{(m)}\frac{(y_i-\mu_Y)^2}{y_i}} \quad (20)$$

and $c^{(m+1)}$ is obtained by numerically solving the equation:

$$0 = n_2^{(m)}\left[\log\frac{\mu_Y}{\Gamma(1-\frac{1}{c})} + \frac{1}{c}\left[1-\psi\left(1-\frac{1}{c}\right)\right]\right] - \sum_{i=1}^{n}\gamma_{i2}^{(m)}\log y_i + \left[\frac{\mu_Y}{\Gamma\left(1-\frac{1}{c}\right)}\right]^c \sum_{i=1}^{n}\gamma_{i2}^{(m)} y_i^{-c}\left[\log\frac{y_i\Gamma(1-\frac{1}{c})}{\mu_Y} + \frac{\psi(1-\frac{1}{c})}{c}\right] \quad (21)$$

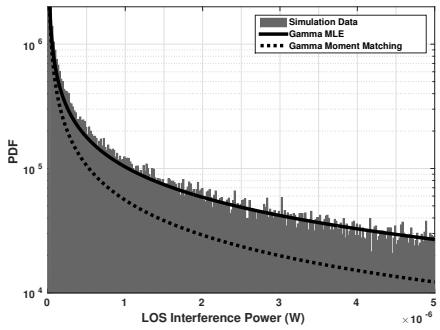

Fig. 1: Sample PDF of LOS interference models at $\alpha_l = 3.5$, $\sigma_l = 4$ dB, ($P_{max} = 30$ dB, $D = 75$ m).

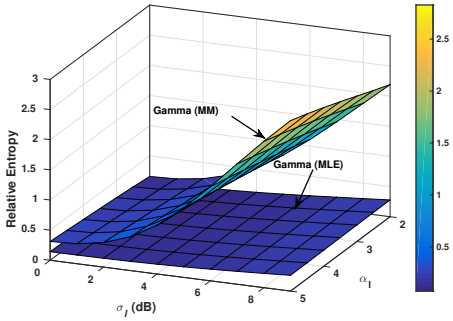

Fig. 2: Relative entropy of LOS interference power models at $D = 75$ m, ($P_{max} = 30$ dBm).

where $n_j^{(m)} = \sum_{i=1}^{n} \gamma_{ij}^{(m)}$.

Proof. Omitted due to space, see [9] for details. □

6. NUMERICAL PERFORMANCE RESULTS

In this section, we use simulation data obtained from the stochastic geometry based network setting in Sec. 2.1 to numerically verify the validity of the proposed interference models. We consider a typical cell of radius $R_0 = 150$ m, which is related to λ_1 as $\lambda_1 = 0.25R_0^{-2}$. We use a fixed value of the path loss intercept $\beta_l = \beta_n = -72.3$ dB.

We first verify the LOS Gamma distribution interference models. In Fig. 1, we show a sample LOS interference power distribution at one antenna element of a UE located at $D = 75$m from the origin for $\alpha_l = 3.5$ and $\sigma_l = 4$ dB. We note that the Gamma MM starts to diverge away from the simulation data at this value of α_l as confirmed in Fig. 2 by plotting the relative entropy [20] versus σ_l and α_l. The Gamma MLE model, on the other hand, provides a very good fit with simulation data with low KL distances.

Next, we compare the NLOS mixture distribution interference model to the Gamma distribution fitted to the simulation data using MLE. We visually confirm from the sample PDF plot in Fig. 3 at $\alpha_n = 3.5$ and $\sigma_n = 4$ dB that the Gamma MLE can no longer approximate the interference power distribution for NLOS components. Instead, the mixture distribution NLOS interference model provides a perfect fit to the simulation data.

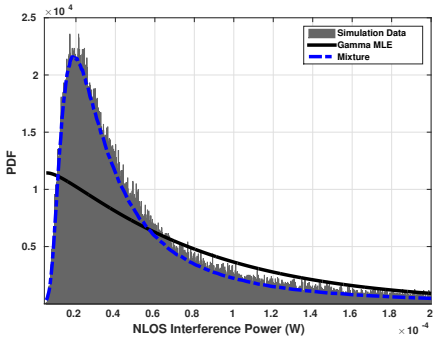

Fig. 3: Sample PDF of NLOS interference models at $\alpha_l = 3.5$, $\sigma_l = 4$ dB, ($P_{max} = 30$ dB, $D = 75$ m).

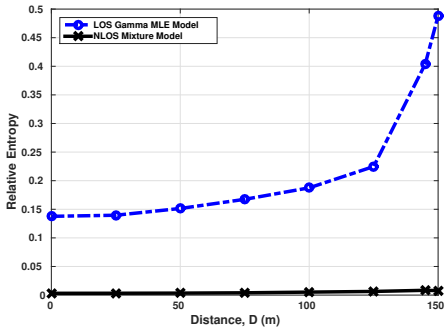

Fig. 4: Relative entropy of LOS and NLOS interference power models versus distance D m, ($\alpha_l = \alpha_n = 3.5$, $\sigma_l = \sigma_n = 4$ dB).

In Fig. 4, we plot the relative entropy of the LOS Gamma MLE and the NLOS mixture distribution interference models at the sample values $\sigma_l = \sigma_n = 4$ dB and $\alpha_l = \alpha_n = 3.5$ versus the considered UE distance D from the origin. We see that for both models, the relative entropy is reasonable compared to a maximum possible KL distance of ∞. The maximum KL distance is 0.488 at the cell edge for the LOS Gamma MLE model and is below 0.02 for the NLOS mixture model, suggesting excellent fits.

7. CONCLUSION

We have introduced a new probabilistic interference model in which the LOS and NLOS interference powers are represented separately as a Gamma distribution and a mixture of the Inverse Gaussian and Inverse Weibull distributions, respectively. The information theoretic based relative entropy (KL distance) metric is exploited to measure the relative distance between the developed interference models and the simulated data. Maximum likelihood estimation of the Gamma distribution provides a much better fit than moment matching. Further, the EM algorithm provides an excellent estimation of the mixture model parameters resulting in the model having a perfect fit irrespective of the receiving node location. As a future work, we plan to verify the proposed model against real measurement data.

8. REFERENCES

[1] S. Rajagopal, S. Abu-Surra, and M. Malmirchegini, "Channel feasibility for outdoor non-line-of-sight mmwave mobile communication," in *IEEE Vehicular Tech. Conf. (VTC Fall)*, Sept 2012, pp. 1–6.

[2] W. Roh, Ji-Yun Seol, and et. al., "Millimeter-wave beamforming as an enabling technology for 5G cellular communications: theoretical feasibility and prototype results," *IEEE Comm. Magazine*, vol. 52, no. 2, pp. 106–113, Feb. 2014.

[3] F Boccardi, R.W. Heath, and et. al., "Five disruptive technology directions for 5G," *IEEE Comm. Mag.*, vol. 52, no. 2, pp. 74–80, Feb. 2014.

[4] Tianyang Bai, Vip Desai, and Robert W Heath, "Millimeter wave cellular channel models for system evaluation," in *IEEE ICNC*, 2014, pp. 178–182.

[5] T. Bai, A. Alkhateeb, and R. Heath, "Coverage and capacity of millimeter-wave cellular networks," *IEEE Comm. Mag.*, vol. 52, no. 9, pp. 70–77, Sept. 2014.

[6] T.S. Rappaport, Shu Sun, and et. al., "Millimeter wave mobile communications for 5G cellular: It will work!," *Access, IEEE*, vol. 1, pp. 335–349, 2013.

[7] T.S. Rappaport, F. Gutierrez, and et. al., "Broadband millimeter-wave propagation measurements and models using adaptive-beam antennas for outdoor urban cellular communications," *Antennas and Propagation, IEEE Trans. on*, vol. 61, no. 4, pp. 1850–1859, April 2013.

[8] M. R. Akdeniz, Yuanpeng Liu, and et. al., "Millimeter wave channel modeling and cellular capacity evaluation," *IEEE Journal on Sel. Areas in Comm.*, vol. 32, no. 6, pp. 1164–1179, 2014.

[9] H. Elkotby and Mai Vu, "Interference modeling for 5G millimeter wave beamforming," *Submitted to IEEE Trans. on Wireless Comm.*

[10] T. Bai and R.W. Heath, "Coverage and rate analysis for millimeter-wave cellular networks," *IEEE Trans. on Wireless Comm.*, vol. 14, no. 2, pp. 1100–1114, Feb 2015.

[11] M.K. Samimi, T.S. Rappaport, and et. al., "Probabilistic omnidirectional path loss models for millimeter-wave outdoor communications," *Wireless Comm. Letters, IEEE*, vol. 4, no. 4, pp. 357–360, Aug 2015.

[12] M. K. Samimi, S. Sun, and T. S. Rappaport, "Mimo channel modeling and capacity analysis for 5g millimeter-wave wireless systems," in *2016 10th European Conference on Antennas and Propagation (EuCAP)*, April 2016, pp. 1–5.

[13] David Tse and Pramod Viswanath, *Fundamentals of wireless communication*, Cambridge university press, 2005.

[14] T. S. Rappaport, G. R. MacCartney, and et. al., "Wideband millimeter-wave propagation measurements and channel models for future wireless communication system design," *IEEE Transactions on Communications*, vol. 63, no. 9, pp. 3029–3056, Sept 2015.

[15] François Baccelli and Bartlomiej Blaszczyszyn, *Stochastic geometry and wireless networks: Theory*, vol. 1, Now Publishers Inc, 2009.

[16] R. S. Chhikara J. L. Folks, "The inverse gaussian distribution and its statistical application – a review," *Journal of the Royal Stat. Society. Series B (Methodological)*, vol. 40, no. 3, pp. 263–289, 1978.

[17] Horst Rinne, *The Weibull distribution: a handbook*, CRC Press, 2008.

[18] C. Walck, "Handbook on statistical distributions for experimentalists," *University of Stockholm Internal Report SUF-PFY/96-01, available from www. physto. se/ walck*, l 2007.

[19] H. Elkotby and Mai Vu, "Uplink user-assisted relaying in cellular networks," *Wireless Comm., IEEE Trans. on*, vol. 14, no. 10, pp. 5468–5483, Oct 2015.

[20] Thomas M. Cover and Joy A. Thomas, *Differential Entropy*, pp. 243–259, John Wiley & Sons, Inc., 2005.